SIMULATION OF MECHANICALLY STIRRED TWO-PHASE LIQUID–GAS FLOW*

Ivan FOŘT[a], Vladimír ROGALEWICZ[b] and Miroslav RICHTER[c]

[a] *Department of Chemical and Food Process Equipment Design, Czech Technical University, 166 07 Praha 6,*
[b] *Research Institute of Plant Production, 161 06 Praha 6 — Ruzyně and*
[c] *Chemopetrol, Spolana Neratovice, 277 11 Neratovice*

Received November 8th, 1984

The study describes simulation of the motion of bubbles in gas, dispersed by a mechanical impeller in a turbulent low-viscosity liquid flow. The model employs the Monte Carlo method and it is based both on the knowledge of the mean velocity field of mixed liquid (mean motion) and of the spatial distribution of turbulence intensity (fluctuating motion) in the investigated system — a cylindrical tank with radial baffles at the wall and with a standard (Rushton) turbine impeller in the vessel axis. Motion of the liquid is then superimposed with that of the bubbles in a still environment (ascending motion). The computation of the simulation includes determination of the spatial distribution of the gas holds-up (volumetric concentrations) in the agitated charge as well as of the total gas hold-up in the system depending on the impeller size and its frequency of revolutions, on the volumetric gas flow rate and the physical properties of gas and liquid. As model parameters, both liquid velocity field and normal gas bubbles distribution characteristics are considered, assuming that the bubbles in the system do not coalesce.

The main purpose of mixing in two-phase gas–liquid systems is to attain a homogeneous spatial distribution of the interface in the whole agitated volume. Under these conditions the mass transfer rate in the whole system (*e.g.* in agitated fermenters, absorbers) does not change and the quality of reaction product is the same during the whole operation. One of the most important causes of the homogeneous spatial distribution of the interface area is the capacity of the impeller to produce an intense two-phase flow in the whole stirred volume. This article is focused on the description of such flow obtained numerically from a computer.

Basic characteristic of the flow of mechanically agitated liquid–gas charge, of the interface area and gas hold-up (volumetric fraction) have been discussed *e.g.* in a number of experimental[1–5,19] and theoretical[6–8] studies. In them, the mentioned dependent variables have been investigated with respect to the influence of all geometric, kinematic and physico-chemical quantities which may affect the nature of a mechanically stirred two-phase liquid–gas flow.

* Part LXVI in the series Studies on Mixing; Part LXV: This Journal *50*, 2863 (1985).

Mathematical model of the flow simulation of two-phase liquid–gas mixture or of the mixture of two immiscible liquids in an agitated system is based on the notion that the dispersed phase is composed of spherical particles of given distribution. Only collisions among two particles are considered. The model takes into account the coalescence, breakage or the formation of unidentical particles chosen at random. Their motion is either random or follows the direction of the continuous (liquid) phase – *i.e.* its local mean velocity vector. In calculating the velocity of a gas particle, the apparent rising velocity of the bubble in the liquid is also taken into account. The investigated system is considered symmetrical around the vessel axis and impeller shaft. The results of[6] make it evident that the local mean velocity vector is supposed to act on the moving gas bubble merely by its direction and not by its absolute value (*i.e.* magnitude). Furthermore, in the calculations the mean gas hold-up is fixed beforehand and accordingly, the offtake of a given amount of gas (*i.e.* bubbles) from the respective depth measured from the surface is arbitrary. Finally, the numerical solution proposed uses carthesian coordinates instead of cylindrical ones, which creates problems in choosing a suitable tank-section containing the cells of a certain network. The same study[6] also lacks a sufficiently detailed investigation of the liquid turbulence, because this quantity is considered only at two levels of its values – that is, just for the two basic subdivisions: the flow from the impeller region and the rest of agitated charge.

The results of experimental investigation of the stirred liquid–gas charge imply that the flow of this mixture may be divided into two regions:

I; The flow close to the impeller blades, where the so-called cavities occur behind them, which are the source of gas dispersion in the liquid flow leaving the region of the rotating impeller[8].

II; The flow in the continuous phase of agitated charge including the circulation with the fed gas and the recirculation in the tank[8].

The observation as well as the measurement of the spatial distribution of local gas hold-up in the volume[2,3,8,9] have shown that the investigated two-phase flow in a cylindical vessel with radial baffles at the wall may – according to the quantity of gas feed – exist in the following forms:

a) little or no gas dispersion,

b) dispersion of bubbles in the upper part of the vessel above the impeller,

c) injected gas recirculates in the upper part of the vessel and its bubbles appear also below the impeller,

d) the gas recirculates both above and below the impeller.

These conditions are attained, unless the impeller is flodded by gas[10], *i.e.* if the energy transferred to the charge does not suffice for the dispersion of the injected gas. Such situation has been experimentally studied and – as in the above case – semi-

empirical relations have been published, characterizing, for a given geometrical configuration of agitated system, the kinematic or dynamic conditions under which the respective form of the two-phase mixture flow occurs.

THEORETICAL

The agitated system considered (see Fig. 1) is a cylindrical vessel with radial baffles of width $b = 0{\cdot}1\ D$ at its wall filled with a low-viscosity liquid up to the height $H = D$. The charge is mixed by a (standard) six-blade disc turbine impeller of diameter d, smaller than the half of vessel diameter D. The impeller axis coincides with that of the vessel. The gas (air) of the volumetric flow rate $\dot{V}_g$ is conducted by a tube directly under the rotating impeller. In the vessel cylindrical coordinate system is introduced, whose origin is in the intersection of the vessel axis and the plane of vessel bottom. The coordinate z (axial coordinate) then coincides with the vessel axis, the coordinate r (radial coordinate) is drawn from the vessel axis to the wall.

For the numerical model (simulation) of the two-phase liquid–gas flow in the defined system the following simplifying assumptions have been considered:

1) The system is axisymmetrical, therefore the influence of angular coordinate in the cylindrical coordinate system need not be taken into account. *2*) The process in the system is quasistationary. *3*) The system is isothermal and the liquid incompressible. *4*) The flow regime of agitated charge is turbulent. *5*) The flow of continuous liquid phase is not influenced by the presence of gas. *6*) The gas dispersion does not coalesce.

The convective flow field is schematically divided into nine regions above and below the horizontal plane of the impeller separating disc[11] (see Fig. 2). The regions are described by a closed system of equations for the mean flow (macroflow) of agitated charge. Starting from the impeller region in the direction of flow* the individual regions are:

^{i}O region of flow from the rotating impeller,
^{i}A region of flow bending at the wall to the bottom (^{1}A) or to the liquid surface (^{2}A),
^{i}B region of ascending (^{2}B) or descending (^{1}B) flow along the wall,
^{i}C region of the flow assuming the radial direction due to the vessel bottom (^{1}C) or the liquid surface (^{2}C),
^{i}D flow region at the bottom or at the liquid surface,
^{i}E region where the radial direction of the flow changes into axial, upwards (^{1}E) or downwards (^{2}E) to the impeller,
^{i}F region of the flow ascending (^{1}F) or descending (^{2}F) along the system axis,

* The regions with the same notation are equivalent, the superscript "1" signifies that the region is under the plane of the impeller separating disc, the superscript "2" signifies the region above this plane.

^{i}G region of irregular flow with insignificant mean velocity components, surrounded by other regions,

^{i}H region in the vicinity of the impeller above the plane of the separating disc (^{2}H) or below it (^{1}H).

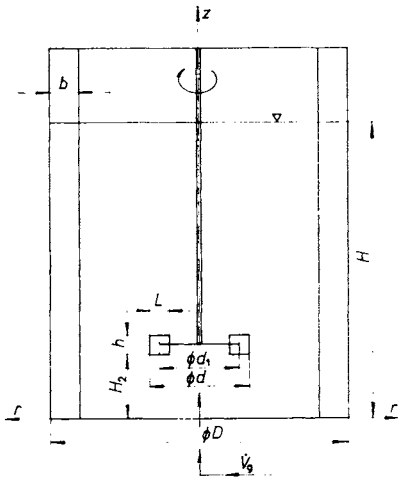

FIG. 1

Agitated vessel with standard turbine impeller and radial baffles

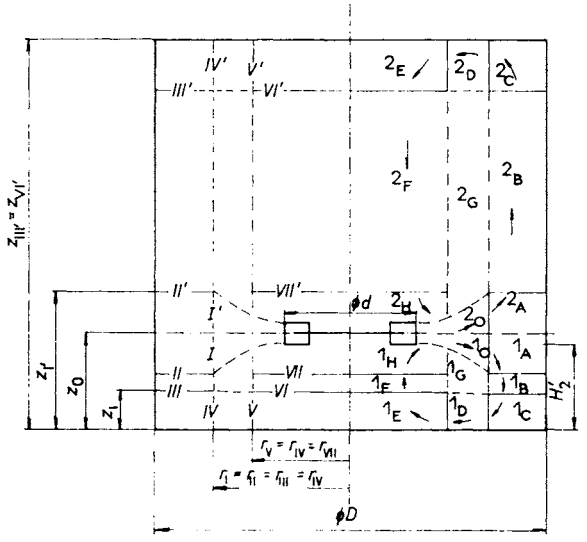

FIG. 2

Distribution of cylindrical vessel with standard turbine and radial baffles into characteristic flow regions ($d/D < 1/2$, $D = H$, $H_2/H \in \langle 1/4; 1/2 \rangle$)

For region ^{i}O, $(i = 1, 2)$ turbulent flow of a viscous incompressible liquid produced by a standard turbine impeller conceived as a cylindrical axisymmetrical tangential jet has been considered[12], in other regions the convective flow is assumed as a potential flow of incompressible liquid. The whole system may then be described by a set of equations[11] expressing the velocity field of the axial $\langle w_{ax} \rangle$ and radial $\langle w_{rad} \rangle$ mean velocity components. Its parameters are mean velocity field characteristics in region ^{i}O, $(i = 1, 2)$[13].

The spatial distribution of the fluctuation velocity component $\langle w'^2 \rangle^{1/2}$ or of its axial and radial components is implied either by the results of direct measurements of turbulence intensity $\langle w'^2 \rangle^{1/2} / \langle w \rangle$[12,14] or by the correlations for the fluctuating component of the velocity[15,16]. For regions ^{i}O, ^{I}A, $(i = 1, 2)$ and for ^{1}H and ^{2}H, if $r < d/2$, the results[12] have been used, for ^{i}B, ^{i}C, ^{i}D, ^{i}E and ^{i}G, $(i = 1, 2)$ relation[15] has been applied

$$\langle w'^{2}_{rad} \rangle^{1/2} = \frac{0{\cdot}511 n d^2}{(D^2 H)^{1/3}} \tag{1}$$

and

$$\langle w'^{2}_{ax} \rangle^{1/2} = \frac{0{\cdot}462 n d^2}{(D^2 H)^{1/3}}, \tag{2}$$

where w'_{rad} and w'_{ax} are the radial and axial components of the fluctuating local velocity of liquid. Rising velocity of gas bubbles in the still (motionless) medium may be written in the form[6]

$$w_{bax} = \frac{4}{9} \frac{g d_b^2}{\eta} (\varrho_l - \varrho_g) f(Hu) \tag{3a}$$

for $d_b \in \langle 2{\cdot}0 - 10^{-4}\ \mathrm{m};\ 1{\cdot}2 \,.\, 10^{-3}\ \mathrm{m} \rangle$, resp.

$$w_{bax} = \sqrt{\left(\frac{2\sigma}{d_b \varrho_l} + \frac{g d_b}{2} \right)} f(Hu) \tag{3b}$$

for $d_b \in \langle 1{\cdot}2 \,.\, 10^{-3}\ \mathrm{m};\ 1{\cdot}0 \,.\, 10^{-2}\ \mathrm{m} \rangle$.

The function $f(Hu)$ in relations (*3a*) and (*3b*) expresses the so-called Marrucci correction for mutual influence of bubbles in the dispersion[17]. It is the function of local gas hold-up value Hu in the form

$$f(Hu) = \frac{(1 - Hu)^2}{1 - Hu^{5/2}}. \tag{4}$$

Actual motion of bubbles in agitated charge is simulated by means: of superimposing

all the following three factors (see Fig. 3): local mean velocity of liquid, local fluctuating components of liquid velocity and the rising velocity of the bubble in still liquid. All the given velocity components are considered in vector from, *i.e.* as vector sums of liquid velocity in the radial and axial direction, the rising velocity of a bubble, however, is taken only in the axial direction towards the liquid surface (this direction being the positive direction of the introduced coordinate system; see Fig. 1).

The motion of the bubble close to the boundaries of the investigated system is depicted in Fig. 4. After reaching the wall or the bottom, the bubble reflects back to

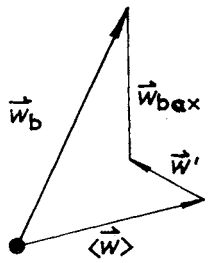

FIG. 3
Calculation of resulting bubble velocity w_b in given place and time

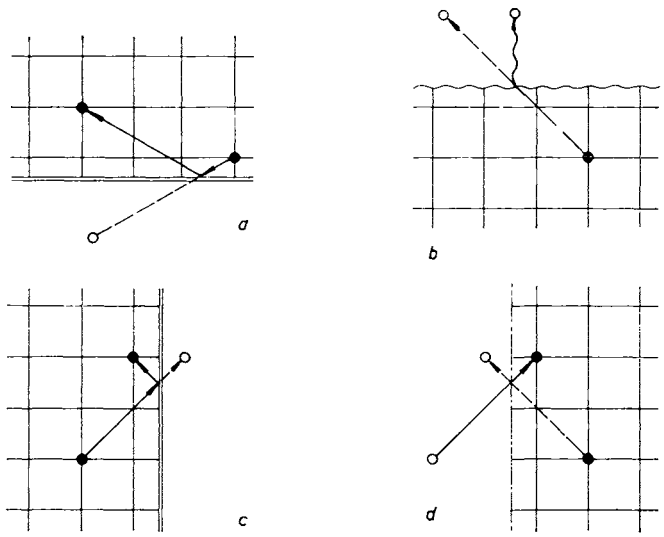

FIG. 4
Simulation of bubble motion at system boundaries. *a* lower boundary (vessel bottom), *b* upper boundary (liquid surface), *c* right boundary (vessel wall), *d* left boundary (vessel symmetry axis)

the vessel according to the law of absolutely elastic body recoil. If its new position is located above the liquid surface, the bubble leaves the system. Consequently, the dispersed particles continually added into the system under the impeller leave the agitated charge through its surface. If the bubble has to pass through the vessel axis, it is assumed (see assumption 1) that other bubble with the same parameters moves from the outside into the investigated volume.

The model for the simulation of the two-phase liquid–gas flow in the agitated system contains three parameters describing the mean flow of the continuous (liquid) phase[13], the spatial distribution of turbulence intensity in the continuous phase[12, 14–16], the relations for the rising velocity of bubbles in the motionless continuous phase (*3*) and (*4*) and two parameters of the normal distribution of spherical bubbles in the dispersed phase of agitated charge[5]: $\langle d_b \rangle$ (average diameter) and σ_{d_b} (standard deviation), resulting from the measured data of the spatial distribution of the local gas holds-up in the investigated system[3].

EXPERIMENTAL

Simulation of the motion of bubbles in the agitated system has been carried out by a computer. Its program models the spatial distribution of bubbles by means of the simulation of motion of all bubbles in the chosen volume. This volume is delimited by two vertical planes intersecting in the symmetry axis of the vessel. With respect to the assumption of its axial symmetry, this volume represents the conditions in the whole system. The part of the system where the simulation is carried out is divided into equal elementary volumes. The position of each of these elements is determined by three coordinates (see Fig. 5) *I*, *J*, *K*, where *K* is the ordinal number of the element with coincident coordinates *I* and *J*, *J* is its distance from the symmetry axis in the radial direction and *I* its distance from the liquid surface, in the axial direction. The set of elements of identical coordinates shall be called a cell. The number of elements in a cell is determined by the ratio of the volume of a given cell to the volume of a cell with $J = 1$. Each element may hold only one gas bubble.

The volume in which the simulation was undertaken was divided into 25 parts in radial and 50 parts in axial directions. Hence, the overall number of elementary volumes was 31 250. For calculation purpose it was assumed that the overall mass of each element (of liquid and gas phases) was located in the centre of gravity (geometrical centre) of the respective cell. Thus individual elements were fully interchangeable, their mass having been placed in the same point.

At the beginning of the calculation (see the flow chart in Fig. 6) necessary input parameters had to be introduced: geometric and kinematic characteristics of the agitated system (D, d, H, H_2', H_2, n), data about the system properties (ϱ_g, ϱ_l, η, σ) and the volumetric flow rate of gas into the system $\dot{V}_g$. For the given conditions of the agitated charge the average bubble diameter $\langle d_b \rangle$ and its standard deviation σ_{d_b} were also given. The program calculates characteristic dimensionless criteria of the process (Re_M, Fr_M and Kp), determines the part of charge and a real time of one iteration. The initial number of bubbles is prescribed and they are distributed homogeneously in the whole system.

The next step is the calculation of velocity field. To each cell five numbers have been alloted: 1 — number of region of the agitated system (see Fig. 2), 2 and 3 — radial and axial liquid mean velocity components in the cell centre, 4 and 5 — radial and axial fluctuation velocity components

in the cell centre. The formation of the block of the input of new bubbles is the first step of each iteration. Always one bubble was added into each cell (to any of its elements) from the centre to the wall, starting at the horizontal level of the impeller separating disc. After filling up all cells, bubbles have been added to higher strata. The addition continues* until the volume of new bubbles has exceeded the determined flow rate. The difference or really supplied gas volume and this flow rate is then subtracted from the determined flow rate for the next iteration.

In the following block the real bubble motion is simulated. The program examines one bubble after another. Their velocity is determined by the sum of three components at a given point (see Fig. 3) and the instant value of their fluctuation component by a random mechanism. The resulting velocity (vector sum of liquid mean velocity, its fluctuation velocity and bubble rising velocity) is divided into its radial and axial components, the real time of an iteration being so determined that neither radial nor axial components of a trajectory travelled by a bubble during one iteration might in any place of the system exceed the triple of the element size in the corresponding direction. After the motion corresponding to the given iteration the new bubble coordinates will not generally coincide with the coordinates of a cell. Therefore a cell out of four neighbouring ones is chosen by a random mechanism, whose coordinate approximates the

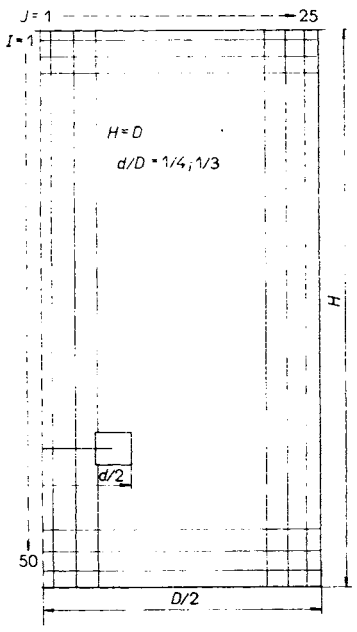

FIG. 5
Discretization (network) of stirred vessel

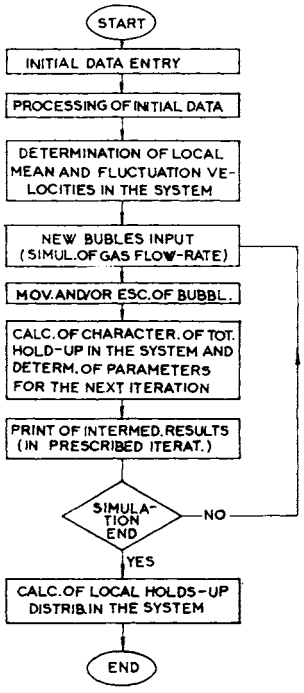

FIG. 6
Flow chart for simulation of bubble motion

* The sizes of individual bubbles have been determined by means of random numbers generator from the known parameters of their distribution.

calculated bubble coordinates most closely, and placed into any of the cell's elements (see Fig. 7). After simulating the motion of all bubbles, the program returns to the block of new bubbles (the iteration number increases by one).

When the number of iterations reaches the prescribed value, the closing block follows (see also Fig. 6). In this block, local hold-up values Hu_{calc} are calculated as spatially averaged values from the cells around the chosen network points, *i.e.* as the mean values of the chosen number of the last iterations realized. Besides, the total hold-up of gas $\langle Hu_{calc} \rangle$ is determined. The obtained calculation results have been recorded.

Whenever the program employed a random mechanism, a generator of pseudorandom numbers has been used. The numbers were distributed uniformly in the interval (0; 1). These numbers X_n were generated by the congruent method according to the relations

$$I_{n+1} = (109 I_n + 3\,393)_{mod\,65\,536}\,, \tag{5}$$

$$X_n = I_n/65\,536 \tag{6}$$

and transformed into the respective distribution[18].

RESULTS AND DISCUSSION

The investigated system, to which the simulation of bubble motion in agitated charge refers, is a cylindrical vessel of diameter D with four radial baffles reaching to the bottom. The baffle width $b = 0{\cdot}1D$. In the vessel axis there is a standard disc turbine impeller with six blades of diameter $d = D/3$ or $d = D/4$, whose height above the bottom is $H'_2 = D/4$. The gas (air) is fed by a tubing in the vessel axis and let under the impeller. The physical properties of agitated charge are: 0·3M solution of Na_2SO_4, $\varrho_l = 1\,031\ kg\,m^{-3}$, $\varrho_g = 1{\cdot}164\ kg\,m^{-3}$, $\eta = 9{\cdot}8 \,.\, 10^{-4}$ Pa s, $\sigma = 0{\cdot}05\ Nm^{-1}$. The geometric parameters are: $D = H = 286$ mm, $b = 28{\cdot}6$ mm, $d = 71{\cdot}5$ mm, $(d/D = 1/4)$, $d = 95$ mm$(d/D = 1/3)$, $H'_2 = 71{\cdot}5$ mm.

The range of calculations was given both by the demand to obtain a set of results of such extent, from which reliable conclusions about the success of the developed simulation program could be made, and by a limiting requirement of the sets of

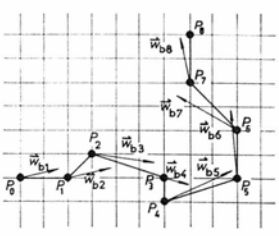

FIG. 7

Bubble motion simulation. P_0 — initial position of bubble, P_i — bubble position after i-th iteration, $\mathbf{w}_{bi}$ — resulting bubble velocity vector after i-th iteration, $P_{i-1} \cdots P_i$ — simulated bubble motion in i-th iteration

experimental data of the spatial distribution of local hold-ups of gas in the system[3,19]. Simultaneously, it was necessary to observe that the stirring intensity and air flow rate would not represent flooding conditions of the mixer[10]. The simulation model has been derived considering the validity of six simplifying assumptions. The first and the third one would not – in principle be necessary to introduce, because the numerical procedure (see *e.g.* Fig. 7) could be extended; even the dependence of physicochemical properties of liquid and gas on temperature could be considered. This, however, would create an enormous demand both on the capacity of computer memory and on calculation time. The application of the solution based on the validity of the above given assumptions is corroborated by its successful use in solving other problems concerning the investigated system[3,11,12,19]. The validity of the second and fourth assumptions is conditioned by the values of $Re_M > 1{\cdot}0 \cdot 10^4$. This condition was fulfilled for all the investigated cases. The sixth assumption, whose introduction again reduces the demands on the scope and length of the program, is fulfilled in the case of mixing of the two-phase gas-liquid charge, the liquid fraction of which is a solution of strong electrolyte[4,7,8]. As the air bubbles moving in the 0·3M solution of Na_2SO_4 behave according to this assumption, it may be considered as fulfilled. The fifth assumption was based on the reasoning that the gas concentration in the liquid does not, even locally, reach such high values that the gas phase might influence the flow and the turbulence of the liquid. This assumption was not fulfilled especially very close to the blades of rotating impeller[9] – namely in region ^iH, (i = 1, 2) and in the inner part of ^iO, (i = 1, 2). Here, the elsewhere valid assumption had to be replaced by introducing the parameters of the normal bubble size distribution $\langle d_b \rangle$ and σ_{d_b} in the whole agitated system, obtained from the experimental results[3]. From the parameter values it may also be concluded that this distribution, expressed in dimensionless form, is identical for all calculated conditions or experiments, for relative standard deviation of bubble size $\sigma_{d_b}/\langle d_b \rangle$ remains within $\pm 15\%$ of the average value ($d/D = 1/3$: $\sigma_{d_b}/\langle d_b \rangle = 0{\cdot}448$; $d/D = 1/4$: $\sigma_{d_b}/\langle d_b \rangle = 0{\cdot}430$) and is independent on the flow rate of gas and the impeller rotational frequency.

From the results of experiments carried out in order to determine the mean gas hold-up in the investigated system with a standard turbine impeller[1] the following relation may be derived

$$\langle Hu_{exp} \rangle = K(P_g/V)^a \, w_0^b n^c \,. \tag{7}$$

With respect to the fact that the superficial velocity of gas w_0 is directly proportional to its volumetric flow rate

$$w_0 = \frac{4\dot{V}_g}{\pi D^2} \tag{8}$$

proportion (7) may – for a constant system size (tank diameter D) – be written

as follows

$$\langle Hu_{exp} \rangle = K_1 (P_g/V)^a \dot{V}_g^b n^c . \qquad (9)$$

In Table I the values of the exponents b and c in Eq. (9) obtained from experimental total gas hold-up measurements[1] are compared with the values of the coefficients

TABLE I

Comparison of exponent b (Eq. (9)) with coefficient m_1 of regression function (Eq. (10a)) and of coefficient c (Eq. (9)) with coefficient m_2 (Eq. (10b))[a]

d/D	$\dot{V}_g . 10^{-3}$ m^3 s^{-1}	m_1 Eq. (10a)	m_2 Eq. (10b)
1/3	—	0·531	—
1/4	—	0·569	—
1/3	0·115	—	0·237
1/3	0·194	—	0·155
1/3	0·366	—	0·161
1/3	0·562	—	0·489
1/4	0·115	—	0·390
1/4	0·194	—	0·449
1/4	0·366	—	−0·025
1/4	0·562	—	1·080

[a] $0{\cdot}45 \leq b \leq 0{\cdot}65$; $0{\cdot}85 \leq c \leq 1{\cdot}08$.

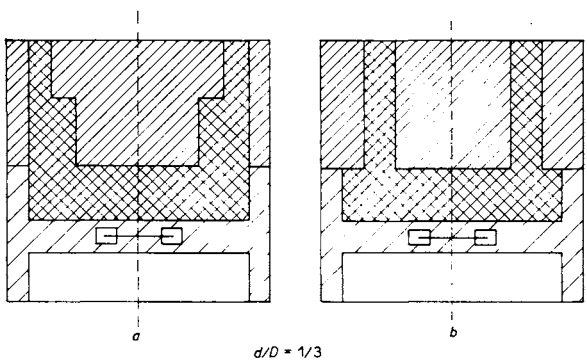

FIG. 8

Spatial distribution of local gas holds-up in liquid agitated by standard turbine impeller. *a* $\langle Hu_{calc} \rangle = 1{\cdot}12\%$; $n = 6{\cdot}67\ s^{-1}$; $\dot{V}_g = 0{\cdot}194 . 10^{-3}\ m^3\ s^{-1}$. *b* $\langle Hu_{calc} \rangle = 0{\cdot}885\%$; $n = 5{\cdot}83\ s^{-1}$; $\dot{V}_g = 0{\cdot}115 . 10^{-3}\ m^3\ s^{-1}$

m_1 in Eq. (*10a*) for varying volumetric flow rate at constant n

$$\log \langle Hu_{\text{calc}} \rangle = C_1 + m_1 \log \dot{V}_g , \quad [d/D = \text{const.}] \qquad (10a)$$

and m_2 in Eq. (*10b*) for varying frequency of revolutions n at constant $\dot{V}_g$

$$\log \langle Hu_{\text{calc}} \rangle = C_2 + m_2 \log n , \quad [d/D = \text{const.}, \dot{V}_g = \text{const.}] \qquad (10b)$$

obtained from calculated mean gas hold-up values $\langle Hu_{\text{calc}} \rangle$.

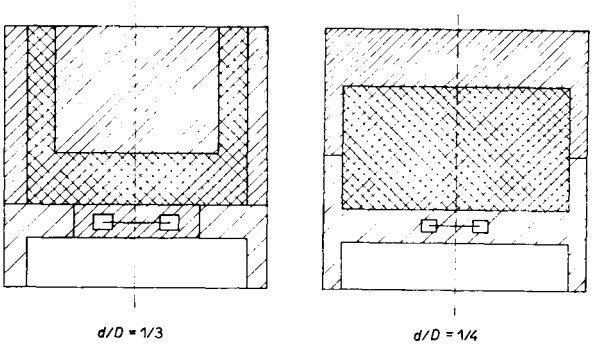

FIG. 9

Spatial distribution of local gas holds-up in liquid agitated by standard turbine impeller. $d/D = 1/3$ — $\langle Hu_{\text{calc}} \rangle = 0{\cdot}95\%$; $n = 6{\cdot}67\ \text{s}^{-1}$; $\dot{V}_g = 0{\cdot}115 \cdot 10^{-3}\ \text{m}^3\ \text{s}^{-1}$. $d/D = 1/4$ — $\langle Hu_{\text{calc}} \rangle = 1{\cdot}11\%$; $n = 10{\cdot}0\ \text{s}^{-1}$; $\dot{V}_g = 0{\cdot}194 \cdot 10^{-3}\ \text{m}^3\ \text{s}^{-1}$

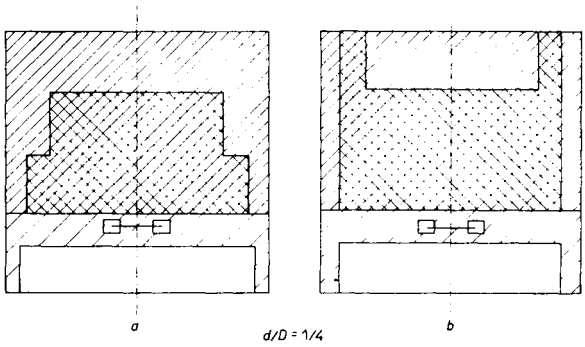

FIG. 10

Spatial distribution of local gas holds-up in liquid stirred by standard turbine impeller. *a* $\langle Hu_{\text{calc}} \rangle = 0{\cdot}851\%$; $n = 8{\cdot}33\ \text{s}^{-1}$; $\dot{V}_g = 0{\cdot}115 \cdot 10^{-3}\ \text{m}^3\ \text{s}^{-1}$. *b* $\langle Hu_{\text{calc}} \rangle = 1{\cdot}15\%$; $n = 11{\cdot}67\ \text{s}^{-1}$; $\dot{V}_g = 0{\cdot}194 \cdot 10^{-3}\ \text{m}^3\ \text{s}^{-1}$

Apparently, the calculated values of m_1 correspond well to the range of b values obtained from experiments. The influence of impeller frequency of revolutions and hence also of the velocity fields of the continuous (liquid) phase on $\langle Hu_{calc} \rangle$ was not, however, found to be so conspicuous, as the experimental results indicate (see Table I, comparison of m_2 and c). This, together with the fact that the calculated values $\langle Hu_{calc} \rangle$ have been found only half as great as the measured ones[7], implies that the used division of the network in the investigated system has been too rough to describe with sufficient precision the motion of bubbles based on the proposed simulation. The better the proposed model will simulate the continuous motion of bubbles, the closer it will answer to the real conditions of the two-phase continuum.

The found dependences of the local holds-up of gas on the impeller frequency of revolutions and the gas volumetric flow rate (see Figs 8–10) confirm – even with respect to the above deviations of calculated and measured values – the results of visual observations[2,8], as well as those of experiments[3,19]. With increasing impeller frequency of revolutions the gas hold-up in the recirculation zone above the impeller and close to the vessel axis of symmetry becomes more aparent. Only after further increase of frequency the gas is penetrated under the rotating impeller *via* the lower circulation loop. With gas flow rate $\dot{V}_g$ increasing, the region of great gas hold-up grows (it is again situated above the impeller and around the vessel axis). With growing flow rate it grows rather in radial direction (region ^{2}G in Fig. 2) than in the axial one (region ^{2}D). At the liquid surface, close to the vessel symmetry axis (region ^{2}E), again a lower value of gas hold-up becomes manifest, apparently due to quick escape of gas through the surface in comparison with the impeller section effect.* Lower concentration of gas in the flow from the impeller region (^{i}O; i = 1, 2) proves the fact that the high value of the radial velocity component in this region[12] causes the flow to drive the bubbles very fast to the vessel wall. Yet the bubbles escape into region ^{2}G, where they rise only due to their buoyancy (see Eqs (*3a*) and (*3b*)) in the field of the random fluctuating component of the continuous phase. Consequently, the distribution of the local holds-up in the charge changes due to the investigated independent variables in keeping with the conclusions of experimental study of the flow of the two-phase liquid–gas charge in the system.

LIST OF SYMBOLS

b	radial baffle width, m
c	molar concentration, mol m^{-3}
D	vessel diameter, m
d	impeller diameter, m
d_b	gas bubble diameter, m

* Additional term of resistance for bubbles leaving the agitated charge through liquid surface, directly proportional to the ratio of inertia and surface forces, can be introduced[20].

$\langle d_b \rangle$	mean gas bubble diameter in agitated charge, m
Fr_M	Froude mixing number ($Fr_M = nd^2/g$)
H	height of still liquid level above vessel bottom, m
H_2	height of lower edge of impeller blades above vessel bottom, m
H_2'	height of impeller separating disc above vessel bottom, m
Hu_{exp}	experimentally determined value of local gas hold-up in charge
Hu_{calc}	calculated value of local gas hold-up in charge
$\langle Hu \rangle$	total gas hold-up in charge
h	height of turbine impeller blade, m
I	axial distance of cell from liquid surface
J	radial distance of cell from liquid surface
K	ordinal number of cell for given I and J
Kp	flow rate criterion ($Kp = \dot{V}_g/nd^3$)
n	impeller frequency, s^{-1}
P_g	gassed impeller power input, W
r	radial coordinate, m
Re_M	Reynolds mixing number ($Re_M = nd^2\varrho_l/\eta$)
$\dot{V}_g$	volumetric gas flow rate into liquid, $m^3\ s^{-1}$
V	volume of agitated charge, m^3
$\langle w \rangle$	resulting liquid mean velocity, ms^{-1}
w_b	resulting velocity of gas bubble, ms^{-1}
w'	fluctuation component of velocity, ms^{-1}
$\langle w_{ax} \rangle$	axial component of liquid mean velocity, ms^{-1}
$\langle w_{rad} \rangle$	radial component of liquid mean velocity, ms^{-1}
w_0	superficial velocity of gas in agitated liquid, ms^{-1}
$w_{b\,ax}$	rising velocity of bubble in still medium, ms^{-1}
z	axial coordinate, m
ϱ_l	density of liquid phase, $kg\ m^{-3}$
ϱ_g	density of gas phase, $kg\ m^{-3}$
η	dynamic viscosity of liquid phase, Pa s
σ	interfacial tension of liquid–gas system, $N\ m^{-1}$
σ_{db}	standard deviation for normal distribution of bubble sizes in charge, m

REFERENCES

1. Vlček J., Steidl E., Kudrna V.: This Journal *34*, 373 (1969).
2. Calderbank P. H.: Trans. Inst. Chem. Eng. *36*, 443 (1958).
3. Wisdom D.: *Thesis*. University of London, London 1974.
4. Machoň V., Vlček J., Kudrna V.: This Journal *43*, 593 (1978).
5. Kawecki W., Reith T., Van Heuven J. W., Beck W. J.: Chem. Eng. Sci. *22*, 1519 (1967).
6. Zeitlin M. A., Tavlarides L. L.: Can. J. Chem. Eng. *50*, 207 (1972).
7. Hughmark G. A.: Ind. Eng. Chem., Proc. Des. Develop. *10*, 638 (1080).
8. Nienow A. W., Wisdom D. J., Middleton J. C.: *The Effect of Scale and Geometry on Flooding, Recirculation and Power in Gassed Stirred Vessels*. Paper presented on the 2nd European Conference on Mixing, Cambridge 1977.
9. Reith K. van't, Smith J. M.: Chem. Eng. Sci *23*, 1994 (1974).
10. Mikulcová E., Kudrna V., Vlček J.: Sb. Vys. Šk. Chemicko-Technol. Praze K *1*, 167 (1967).
11. Fořt I., Obeid A., Březina V.: This Journal *47*, 226 (1982).

12. Drbohlav J., Fořt I., Máca K., Ptáček J.: This Journal *43*, 3148 (1978).
13. Fořt I., Möckel H. O., Drbohlav J., Hrach M.: This Journal *44*, 700 (1979).
14. Fořt I., Hrach M., Obeid A.: Sb. Vys. Šk. Chemicko-Technol. Praze K *15*, 37 (1980).
15. Schwartzberg H. G., Treybal R. E.: AIChE J. *7*, 1 (1968).
16. Günkel A. A., Weber M. E.: AIChE J. *21*, 931 (1975).
17. Marucci G.: Ind. Eng. Chem., Fund. *4*, 224 (1965).
18. Sobol I. M.: *Numerical Monte Carlo Methods* (in Russian). Nauka, Moscow 1973.
19. Nagase Y., Yasui H.: Chem. Eng. J. *27*, 37 (1983).
20. Fořt I., Rogalewicz V.: *Simulation of Gas–Liquid Flow in Agitated Charge.* Paper presented at the Xth Engineering Foundation Conference on "Mixing". Henniker (New Hampshire) 1985.

Translated by M. Procházka.